Exploring the impact of CMIP5 model biases on the simulation of North Atlantic decadal variability

Menary, M. B., Hodson, D. L. R. ORCID: https://orcid.org/0000-0001-7159-6700, Robson, J. I. ORCID: https://orcid.org/0000-0002-3467-018X, Sutton, R. T. ORCID: https://orcid.org/0000-0001-8345-8583, Wood, R. A. and Hunt, J. A. (2015) Exploring the impact of CMIP5 model biases on the simulation of North Atlantic decadal variability. Geophysical Research Letters, 42 (14). pp. 5926-5934. ISSN 0094-8276 doi: 10.1002/2015GL064360 Available at https://centaur.reading.ac.uk/40632/

Exploring the impact of CMIP5 model biases on the simulation of North Atlantic decadal variability

Matthew B. Menary[1,2], Daniel L. R. Hodson[2], Jon I. Robson[2], Rowan T. Sutton[2], Richard A. Wood[1], and Jonathan A. Hunt[3]

[1]Met Office Hadley Centre, Met Office, Exeter, UK, [2]NCAS-Climate, University of Reading, Reading, UK, [3]Department of Earth Sciences, University of Oxford, Oxford, UK

Abstract Instrumental observations, paleoproxies, and climate models suggest significant decadal variability within the North Atlantic subpolar gyre (NASPG). However, a poorly sampled observational record and a diversity of model behaviors mean that the precise nature and mechanisms of this variability are unclear. Here we analyze an exceptionally large multimodel ensemble of 42 present-generation climate models to test whether NASPG mean state biases systematically affect the representation of decadal variability. Temperature and salinity biases in the Labrador Sea covary and influence whether density variability is controlled by temperature or salinity variations. Ocean horizontal resolution is a good predictor of the biases and the location of the dominant dynamical feedbacks within the NASPG. However, we find no link to the spectral characteristics of the variability. Our results suggest that the mean state and mechanisms of variability within the NASPG are not independent. This represents an important caveat for decadal predictions using anomaly assimilation methods.

1. Introduction

Initial conditions within the North Atlantic subpolar gyre (NASPG) have been shown to be important in making skilful decadal forecasts [*Dunstone et al.*, 2011]. However, even when given similar initial conditions, decadal predictions of the North Atlantic between different models can be quite different [*Pohlmann et al.*, 2013]. Indeed, decadal variability in the North Atlantic Ocean, although extensively investigated in both coupled and uncoupled models [e.g., *Eden and Willebrand*, 2001; *Dai et al.*, 2005; *Dong and Sutton*, 2005; *Cabanes et al.*, 2008; *Alvarez-Garcia et al.*, 2008; *Biastoch et al.*, 2008], is still poorly understood, in part due to the paucity of constraining observational data [*Good et al.*, 2013].

An array of coupled, partially coupled, and ocean-only mechanisms have been proposed to describe simulated variability in the NASPG (see above references and *Liu* [2012] for a review), while the pacemaker of this variability has been attributed to a variety of processes such as Rossby wave propagation [*Sévellec and Fedorov*, 2013], mean advection timescales [*Delworth et al.*, 1993], and interaction with the deep flow [*Eden and Willebrand*, 2001]. Despite the large number of postulated mechanisms and key processes, a periodicity of around 20 years has begun to emerge as the common timescale of simulated multiannual/decadal variability in the NASPG [*Frankcombe et al.*, 2010], consistent with some high-resolution paleorecords in this region [*Sicre et al.*, 2008; *Chylek et al.*, 2012]. This timescale describes variability generally confined to the subpolar gyre, with feedbacks to other regions in the Arctic and/or subtropical North Atlantic usually involving longer timescales [*Jungclaus et al.*, 2005; *Menary et al.*, 2012].

Within the NASPG, a key region in most mechanisms of decadal (or longer) variability is the deep water formation (DWF) region of the Labrador Sea, where surface signals can spread to depth and impact the large-scale dynamics of the region [*Medhaug et al.*, 2012], though we note that some models can locate their main DWF regions elsewhere [*Ba et al.*, 2014]. Similar to the disparate mechanisms of variability, although models generally agree that the Labrador Sea (or model equivalent) is important, they are split on whether decadal timescale changes in density in this region are controlled by either temperature or salinity.

In summary, there remain many systematic differences across the present generation of climate models in their representation of North Atlantic decadal variability. We hypothesize that these differences may in part be related to the relationship between mean state biases in the NASPG and whether temperature or salinity

control density changes. This would have ramifications for situations in which mean state biases and the evolution of the system are assumed to be independent, such as decadal forecasts using "anomaly assimilation." In this study, we test the validity of this simple hypothesis linking mean state temperature and salinity biases with the controller of density variability and investigate whether this has implications for the manifestation of decadal variability in the NASPG.

2. Methods/Models

Phase 5 of the Coupled Model Intercomparison Project (CMIP5) represents a coordinated approach to simulating global climate under a variety of scenarios [*Taylor et al.*, 2012]. We examine 40 preindustrial control simulations from 40 individual models from the CMIP5 archive (supporting information Table S1). We use control simulations in all cases to isolate the internal variability while their length allows us to maximize the signal-to-noise ratio for each model (supporting information Table S1). In addition, we examine two iterations of the latest high-resolution coupled climate model from the Met Office Hadley Centre: "HadGEM3" (which comprises Global Atmosphere (GA) version 3.0 [*Walters et al.*, 2011] and the NEMO ocean model version 3.2 [*Madec*, 2008]) [see *Duchez et al.*, 2014, and references therein] and "GC2" (which comprises GA6.0 and NEMO version 3.4 [*Williams et al.*, 2015]). The versions of HadGEM3 and GC2 we analyze are control simulation runs with interannually constant forcings appropriate for the years 2000 and 1850, respectively. We compare the simulations to optimally interpolated observations from the EN4 data set [*Good et al.*, 2013]. We use EN4 data from the most well-observed period 1960–2014 but note that due to undersampling, we have far more confidence in the estimation of the time mean values than the interannual/decadal variability.

All models are regridded on to a regular $1 \times 1°$ horizontal grid to aid analysis. Testing with HadGEM3 and GC2 (not shown), using both original and regridded data, suggests that regridding has very little impact on our subsequent results. The original vertical discretizations are left unaltered. Additionally, all models are linearly detrended prior to analysis, but this again has little effect on our results (not shown). Unless otherwise stated, top 500 m depth-averaged annual mean data are used.

3. Results

3.1. Biases

Models exhibit a wide variety of temperature and salinity (T/S) biases in the northern North Atlantic, a selection of which are shown in Figure 1a for the western SPG (for the full ensemble and wider NASPG see supporting information Figure S1). Both the magnitude and spatial structure of the bias vary greatly, up to $\pm 4°C$ and ± 1 practical salinity unit (psu) for top 500 m depth-averaged temperature and salinity, respectively. Models from the same institution often share similar biases, perhaps associated with a reduction in the effective number of degrees of freedom of our sample [*Knutti et al.*, 2013], but this is not always the case (e.g., IPSL-CM5A-LR and IPSL-CM5B-LR or GISS-E2-H and GISS-E2-H-CC).

In addition to the mean state biases, interannual variability in the northern North Atlantic (as diagnosed by the annual standard deviation) varies from model to model. Figure 1b highlights the combination of mean state biases (compared to EN4) and interannual variability for the volume-averaged Labrador Sea (55–65°N, 45–65°W, top 500 m) across the entire 42-model ensemble. For each model, simulated interannual standard deviations in temperature and salinity are approximately 0.5°C and 0.1 psu, respectively, significantly smaller than the intermodel spread in mean state temperature and salinity. In general, there is a positive correlation between temperature and salinity biases ($r = 0.85$) to the extent that biases are largely density compensated, which holds throughout the NASPG (not shown). However, a small density bias remains, which is typically due to the salinity biases; i.e., models which are warmer and saltier (Figure 1b, top right) are also generally denser than models which are cooler and fresher (Figure 1b, bottom left). The origin of this covariability is unclear, but it is consistent with important roles for either evaporation, deep convection (as the subsurface Labrador Sea is warmer/saltier than the surface), or ocean dynamics (see section 4).

3.2. Density Control

One of the key uncertainties in climate model simulations of the North Atlantic region is whether these simulations imply that the density changes associated with DWF are temperature or salinity controlled. Although individual convective events are likely due to rapid wind-induced cooling (rather than salinifying) of surface waters during wintertime, the frequency and/or intensity of these events depends on both the background
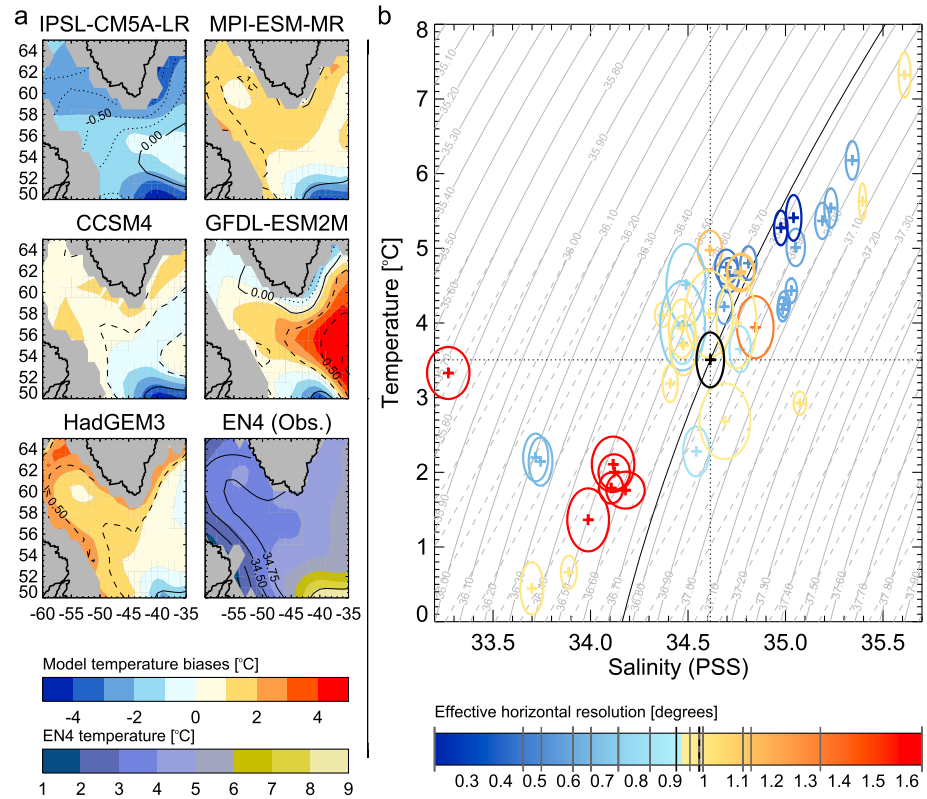
Figure 1. (a) Top 500 m depth-averaged time mean temperature (colors) and salinity (contours) biases in an arbitrary subset of the models, relative to EN4. Salinity contours are solid for zero bias, dotted for negative bias, and dashed for positive bias, with a contour interval of 0.25 psu. Time mean absolute values in EN4 are also shown for comparison. The full model ensemble is shown in the supporting information Figure S1. (b) Top 500 m depth-averaged temperature and salinity mean (crosses) and annual ±1 standard deviation range (ellipses) in the Labrador Sea for the model control simulations (colors) and observations (EN4, black). All time series linearly detrended prior to computing the standard deviation. Contours of constant potential density (relative to 2000 m) are also plotted (grey, solid). A linear fit to these contours, taken when $T = 5°C$ and extrapolated for cooler temperatures, is shown to highlight the nonlinear nature of the seawater equation of state (grey, dashed). The black contour highlights the mean density in EN4. The models have been colored by their effective horizontal resolution in the NASPG, the exact values of which have been indicated in grey on top of the color bar (see section 3.4; note that some resolutions occur more than once) along with the mean resolution (black, solid) and median resolution (black, dashed).

mean and interannual variability of temperature and salinity profiles. As such, both temperature and/or salinity could plausibly be said to control interannual variability in density changes associated with DWF in the Labrador Sea.

In order to quantify whether temperature or salinity is controlling density changes in the Labrador Sea in our 42-model ensemble, we follow the decomposition of *Delworth et al.* [1993] and decompose density changes into those due to temperature and those due to salinity (equation (1)). This assumes a linear decomposition of the nonlinear equation of state, but we suggest that this is not a bad assumption given the small size of interannual T/S variability for any given model (cf. Figure 1b), and indeed, the linear reconstruction explains >96% of the annual variance in density in all models. We then regress the original annual mean density time series (ρ) against those where only temperature or salinity is varying (ρ_T and ρ_S, respectively) to estimate the amount by which temperature or salinity variations are controlling density changes ($\rho_{T\text{control}}$ and $\rho_{S\text{control}}$, respectively):

$$\rho = \rho(T, S, p)$$
$$\rho_T = \rho(T, \bar{S}, p), \quad \rho_S = \rho(\bar{T}, S, p)$$
$$\rho_{T\text{control}} = \text{regr}[\rho, \rho_T], \quad \rho_{S\text{control}} = \text{regr}[\rho, \rho_S] \tag{1}$$

where overbars represent time mean quantities, p is pressure (although we take depth averages), and regr means to take the regression coefficient between two time series. Finally, in order to compare the
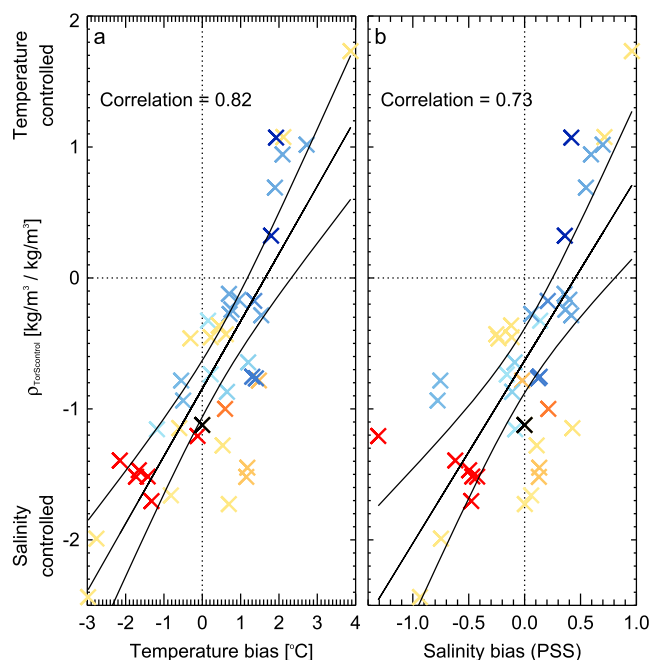
Figure 2. Top 500 m depth-averaged (a) temperature and (b) salinity biases in the Labrador Sea against a measure of the controller of interannual density changes in the Labrador Sea ($\rho_{TorScontrol}$). The colors represent each model's effective horizontal resolution in the NASPG, as in Figure 1b. An estimate of $\rho_{TorScontrol}$ for EN4 has also been added (with zero bias, black). Regression slopes are computed by ordinary least squares regression with the envelope representing an estimate of the 95% confidence interval on the slope.

contributions of temperature and salinity for each model, we difference these two regression slopes to determine a single number: the degree of temperature or salinity control of Labrador Sea density changes, where positive implies greater temperature control (equation (2)):

$$\rho_{TorScontrol} = \rho_{TControl} - \rho_{SControl} \qquad (2)$$

Figure 2 compares the degree of T or S control ($\rho_{TorScontrol}$) with the biases in the Labrador Sea. There are strong correlations between the biases and what controls density changes with regression slopes significantly different from zero. Density changes in warm and salty models appear to be dominated by variability in temperature, whereas density changes in cool and fresh models appear to be dominated by variability in salinity; i.e., T/S biases appear to explain what controls interannual density variability in models and explain to a large extent the spread in the literature on this topic. This can be understood by comparison to Figure 1b in which the potential density contours have been overlaid. For temperatures less than 5°C a linear fit to the density equation (extrapolated from $\rho = \rho(T = 5, S)$) has also been added to highlight the nonlinear nature of the seawater equation of state. A given salinity change has a larger effect on density when the temperature is cool than when it is warm. Similarly, when the background mean temperature is warm, a given temperature change is now more likely/able to play an important role than when it is cool. Note also that although *mean* density biases are due to salinity, it is the combination of both temperature and salinity biases which systematically affect the controller of density *variability*. We find that this result holds for both unfiltered (but detrended) time series representing interannual relationships as well as filtered time series (removing periods less than 5 years) investigating decadal relationships. Indeed, even estimating the relationships on "multidecadal" timescales (by filtering to remove periods less than 30 years) has little effect (not shown); i.e., it is not the case that temperature variability dominates on interannual timescales and salinity variability dominates on decadal timescales.

Despite the above analysis, it is also possible that the magnitude of temperature or salinity interannual variability across models varies with the biases and thus affects what we estimate controls density variability. To determine whether the magnitude of the variability is an important predictor of density control, we scale the T/S variability and repeat our analysis (supporting information Text S1 and Figure S2). Although T/S variability
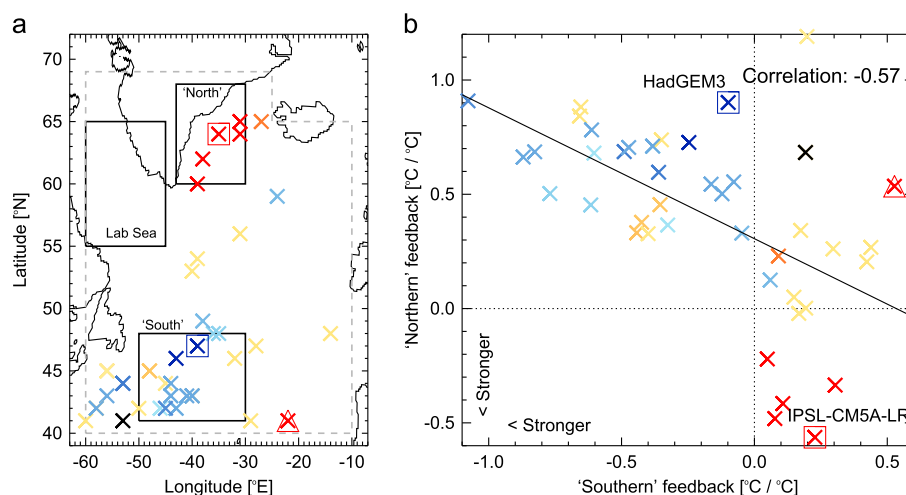
Figure 3. (a) The location, constrained to be within the grey dashed boundary, of the maximum negative correlation with the Labrador Sea depth-averaged temperature (T500, marked region) in each model. The map lags the Labrador Sea index by 1 year; annual, detrended data are used. (b) The location and strength of feedbacks involving the Labrador Sea, estimated by regressing T500 in the Labrador Sea against a "northern" and "southern" index, as described in the text and marked on the map, for the models (colors) and EN4 (black). The trend line and correlation are estimated using a Bayesian approach to total least squares (TLS) regression [*Kelly*, 2007] with the uncertainty on the individual regression slopes for each model used as the measurement errors within the TLS calculation. The HadGEM3 and IPSL-CM5A-LR models have been highlighted with squares and the IPSL-CM5B-LR model with a triangle (see text). The colors represent each model's effective horizontal resolution in the NASPG, as in Figure 1b.

correlates with $\rho_{TorScontrol}$, we find that the magnitude of T/S variability is unlikely to causally affect $\rho_{TorScontrol}$ and suggest that the causation is more likely to be in the opposite direction.

In summary, it appears that simulated Labrador Sea mean state T/S biases do appear to be related to whether interannual/decadal density changes are temperature or salinity controlled. The final question we investigate is whether these mean state biases—and their apparent relationship to what controls density variability—have a systematic impact on the mechanisms of variability within the North Atlantic.

3.3. Labrador Sea Feedbacks

The Labrador Sea has been shown to be an important region in differing mechanisms of decadal variability in the North Atlantic [*Danabasoglu*, 2008; *Escudier et al.*, 2013]—here we examine whether these differences can be simply understood by investigating negative feedbacks associated with depth-averaged temperature anomalies (denoted T500) in the Labrador Sea. That is, when it is anomalously warm/cold in the Labrador Sea, where (if anywhere) in the ocean do the anomalies that reverse the state of the Labrador Sea originate. We use depth averages over the top 500 m for comparison with our previous analysis and because these have a high signal-to-noise ratio. We focus on negative feedbacks as these are required in order to create significant periodicity in the absence of periodic forcing but limit our analysis to the ocean. Indeed, we make no a priori assumptions about the precise details of the feedback mechanism, be it coupled or ocean only. We use temperature (rather than, for example, salinity) for simplicity but note that whatever the mechanism, Labrador Sea DWF is likely to leave signals in both temperature and salinity.

Figure 3a shows the location of maximal negative correlation of T500 with the marked Labrador Sea region at a lag of 1 year (i.e., the map lags the Labrador Sea index by 1 year). A lag of 1 year is used to reduce the confounding effect of the North Atlantic Oscillation (NAO) forcing both the Labrador Sea and the rest of the NASPG simultaneously. The location of this negative correlation follows a curve broadly consistent with the shape of the NASPG. These anomalies propagate into the Labrador Sea and reverse the sign of the initial anomaly (not shown) over the course of a few years to a decade with the timescales varying from model to model (see also section 4). Many models exhibit their maximal negative correlation in the North Atlantic Current region, whereas some show a preference for the East Greenland Current (consistent with elements of the mechanism, though not the specific timescales, of *Escudier et al.* [2013]).

To quantify the differences highlighted in Figure 3a, we design two metrics that aim to characterize these negative feedbacks in ocean temperatures: the magnitude of the (negative) regression gradient between the Labrador Sea index and an index of the North Atlantic Current region (30–50°W, 41–48°N: "south") and the magnitude of the (negative) regression gradient between the Labrador Sea index and an index of the East Greenland Current region (30–45°W, 60–70°N: "north"). It can be seen from Figure 3b that, in general, models have a preference for one feedback or the other, with a stronger northern feedback implying a weaker southern one, and vice versa. The correlation between the two feedbacks is −0.56, which rises to −0.71 when using zero lag (supporting information Figure S3). This method of analysis is also consistent with the individual simulations investigated in previous work where the southern and northern portions of the NASPG were important in HadGEM3 and IPSL-CM5A-LR [*Escudier et al.*, 2013] respectively (highlighted in the figure). Note also the low-resolution outlier IPSL-CM5B-LR (triangle), which has improved tropical atmospheric dynamics compared to IPSL-CM5A-LR but a severely worsened representation of the North Atlantic Ocean with a control Atlantic overturning strength of 4 Sverdrups [*Dufresne et al.*, 2013].

To compare against reality, we add an observational estimate of the feedback using the years 1960–2014 from EN4. The observations occupy a zone where neither a northern nor southern feedback dominates, according to our analysis. This may be because interannual/decadal variability in the observations during this period is also related to a number of other factors, including Great Salinity Anomalies [*Dickson et al.*, 1988], recent rapid warmings of the subpolar gyre [*Robson et al.*, 2012], and possibly a larger role for the NAO [*Scaife et al.*, 2011], to name but a few. Unfortunately, the confounding influence of transient climate change, along with a much shorter record (there are only sporadic observations in the northern North Atlantic prior to 1960), inhibits detailed comparison (see section 4). Nevertheless, the observational estimate lies within the simulated ranges implying that the observed North Atlantic variability may be a sample from the model mechanisms.

3.4. Resolution

The refinement of horizontal resolution in the ocean to permit and even resolve eddies/Rossby waves may be particularly important for regions such as the Labrador Sea [*Gelderloos et al.*, 2011; *Marzocchi et al.*, 2015]. To account for nonregular grids, we estimate the effective resolution of each model in the North Atlantic region (40–76°N, 0–65°W) by simply counting the number of grid cells with centers within this domain on each model's native grid. These range from 1.6° for the IPSL and CMCC models to 0.21° for the new Hadley Centre models (though note that the new Hadley Centre models are post-CMIP5 models).

The effective resolution of the models does appear to show a broad relationship to their biases, with warm and salty models also being of higher resolution than cool and fresh models (Figure 1b). Interestingly, the effective resolution does not appear to correlate with the absolute value of the bias; i.e., higher-resolution models cannot be said to be "better," in terms of their depth-averaged T/S biases in the Labrador Sea, than lower resolution models. In addition, we find that higher-resolution models are more likely to show temperature-controlled interannual/decadal density changes, whereas these density changes are more likely to be salinity controlled in lower resolution models (Figure 2). Lastly, models which have a lower effective resolution in the North Atlantic are much more likely to exhibit signals indicative of a northern feedback than models of higher resolution (Figure 3); this selection between northern and southern feedbacks is not as clear when coloring by $\rho_{TorScontrol}$ (not shown). Possible reasons for the relationship between biases and resolution are discussed next (section 4).

4. Discussion

We have demonstrated, across a 42-member coupled model ensemble, that mean state T/S biases in the North Atlantic covary and are almost density compensating. We have shown that these biases also appear to affect what controls interannual/decadal density variability in the sinking regions, a result that perhaps helps to explain the spread in the literature on this point. Furthermore, we have highlighted how these models appear to favor Labrador Sea feedbacks either to the north or the south. Lastly, the relationships between all of these metrics show some separation by the models' effective horizontal resolution.

A key remaining question is whether there is a further systematic link between the mechanisms of simulated variability and the inherent timescales of this variability. Of the 42 models tested, 26 show a peak in their power spectrum (above the 95% level for that estimated for a similar first-order autoregressive red noise process) for top 500 m volume-averaged temperatures in the NASPG (45–62°N) at short "decadal" timescales (periods of 10–40 years). This rises to 29 models when considering just the Labrador Sea region. Despite this,

we find no relationships between the aforementioned mechanisms/density control and either the preferred timescales or relative magnitudes of decadal variability. Thus, within the statistical power of our reduced sample, there appears to be no systematic relationship between the mechanisms that we have investigated and the subsequent manifestation of decadal periodicity in the North Atlantic subpolar gyre. This is further evidenced by the similar periodicities in HadGEM3 (17 years, not shown) and IPSL-CM5A-LR (20 years) [*Escudier et al.*, 2013] despite very different resolutions/biases/density control. However, it is still possible that there exist systematic relationships on longer timescales, which we have not investigated, perhaps involving the AMOC. Finally, recent work has suggested that observed and simulated (in historical simulations) bidecadal variability in the NASPG may be pace set by volcanic forcing [*Swingedouw et al.*, 2015]. Although the authors find similar timescales of variability, this appears to arise by different mechanisms across the models and further highlights the apparent independence of the mechanisms and overall timescales in the NASPG.

The relationship between the mean T/S (biases) and density control suggests that the real world may be in a state where Labrador Sea annual density variability is controlled by salinity (rather than temperature) changes, similar to lower resolution models (Figure 2). However, there is limited spatial and temporal sampling within the Labrador Sea, particularly during the important wintertime period (defined here as December to February inclusive). For example, there are multiple years in the 1990s in EN4 where there are less than two combined T/S observations below the surface anywhere in the Labrador Sea during winter (not shown). Additionally, it is likely that there has been significant external forcing within this time period, noted in section 3.3. Therefore, we have more confidence in the first-order moments (i.e., the mean, from which we estimate the model biases) than second-order moments (i.e., the observed interannual/decadal variability) and as such we suggest some caution in interpreting measures relating to the observed Labrador Sea variability (cf. black crosses in Figures 2 and 3).

Although it is clear that the effective horizontal resolution of the models in the NASPG is related to their mean state biases, it is not as apparent why this is. We speculate that this relationship may arise due to higher resolution allowing better representation of the strength of boundary currents [*Grotzner et al.*, 1998; *Gelderloos et al.*, 2011], which are an important component of the AMOC [*McCarthy et al.*, 2015], as well as heat transport in the NASPG. The computational overhead of calculating the AMOC streamfunction on the various model grids, and the mixed availability of the streamfunction diagnostic on the CMIP5 archive, precluded direct comparison to the AMOC. However, the zonal mean northward geostrophic circulation at 45°N (depth averaged between 100 and 1000 m) was calculated using the T/S data, which show an interannual correlation with the AMOC time series (maximum at 45°N) of $r = 0.7$ in HadGEM3. This geostrophic estimate was then calculated for all models and used as a proxy for the AMOC. There exist weak correlations between this AMOC proxy and the T/S biases in the NASPG (45–62°N) of $r = 0.46$ (for both temperature and salinity biases), with stronger northward circulation implying warmer and saltier conditions in the North Atlantic across models, consistent with recent multimodel work investigating larger-scale biases [*Zhang and Zhao*, 2015]. It has also been shown that the timescales of the relationship between increased Labrador Sea (or elsewhere) convection and the response of the AMOC can vary greatly between models [*Huang et al.*, 2014], which may also explain the lack of a systematic link between the mechanisms and periodicity of simulated decadal variability, but further analysis is required.

The models we have analyzed are intended to represent a stable climate not undergoing transient climate change. Due to the large role of AMOC-related northward heat transport, combined with uncertainties in AMOC projections, it is not clear whether the North Atlantic subpolar gyre region will actually become warmer or cooler under future climate change [*Collins et al.*, 2013]. Whatever the sign, given that according to our analysis a change in mean T/S could affect the dominant mechanisms of decadal variability (e.g., Figure 2), this implies that the prevalent mechanisms of decadal variability in the NASPG could be different under future climate change.

These results have clear implications for decadal predictions using the common method of anomaly assimilation in which observed oceanic T/S anomalies are assimilated into a climate model's (biased) mean state. The simulated evolution of these anomalies within the climate model is then assumed to be independent of the mean state biases—an assumption that we have shown appears not to be valid when considering the mechanisms of variability. Although a process-based understanding of the mechanisms of North Atlantic decadal change—gained by confronting climate predictions with recent observations—could validate and constrain models, an in-depth understanding of control simulations will still be invaluable to put those results into a

wider context. Until such a time as real world NASPG decadal variability is fully sampled, we recommend a twin strand approach of analyzing multicentury integrations with stable coupled climate models and assessing the hindcast skill of decadal prediction systems.

5. Conclusions

Climate models and direct and indirect observations have highlighted evidence of significant decadal variability within the North Atlantic subpolar gyre (NASPG). Given the paucity of direct observations, it is not clear how the signature of this variability evolves, in either space or time, while model simulations suggest a wide range of disparate mechanisms, many of which involve an important role for the Labrador Sea. To investigate these issues, we have analyzed the systematic relationships across an exceptionally large ensemble of present-generation coupled climate models. We find that

1. Mean state biases in near-surface (top 500 m depth-averaged) temperature and salinity in the Labrador Sea covary, with warm models also being saltier. Ensuing density biases are mostly due to salinity (rather than temperature).
2. There exists a systematic relationship between whether density changes associated with variability in the Labrador Sea are temperature or salinity controlled and the mean state biases. Models that are too cool/fresh tend to have salinity-controlled density variability, whereas models that are too warm/salty tend to show a greater degree of temperature control. This relationship is seen for both interannual and decadal timescale variability.
3. Negative feedbacks with the Labrador Sea tend to fall into two groups that exist either to the north (around the East Greenland Current) or to the south (around the North Atlantic Current). These feedback locations suggest that some of the intermodel spread in decadal variability in the NASPG is related to differences in the preferred feedback location and mechanism.
4. The effective horizontal resolution in the North Atlantic (ranging from 0.21° to 1.6° in our sample) shows some relationship to the mean state biases, density control, and dominant feedbacks. Higher-resolution models are generally too warm and salty, whereas lower resolution models are too cool and fresh in the Labrador Sea. However, there is no relationship between the effective resolution and the absolute magnitude of the biases, suggesting that higher-resolution models cannot be considered to be better than lower resolution models, in terms of their depth-averaged biases in the Labrador Sea.
5. Although there are systematic relationships between biases, density control, and feedbacks, these do not appear to result in systematic relationships with the spectral characteristics of the variability in either the Labrador Sea or wider NASPG. This is consistent with work analyzing HadGEM3 (not shown) and IPSL-CM5A-LR [*Escudier et al.*, 2013] that found different mechanisms but similar periodicities.

Although the mechanisms of NASPG variability cannot be shown to be a systematic predictor of the periodicity, within the statistical power of our ensemble, our results nevertheless suggest that mean state biases influence the characteristics of decadal variability. This implies potential problems for decadal prediction systems that use the methodology of anomaly assimilation, in which the mean state and evolution of the system are assumed to be independent [*Robson*, 2010]. Indeed, the range in individual model biases and mechanisms suggests caution when making decadal predictions using any given model, whether "full-field" or "anomaly assimilating."

References

Alvarez-Garcia, F., M. Latif, and A. Biastoch (2008), On multidecadal and quasi-decadal North Atlantic variability, *J. Clim.*, *21*(14), 3433–3452.

Ba, J., et al. (2014), A multi-model comparison of Atlantic multidecadal variability, *Clim. Dyn.*, *43*(9–10), 2333–2348.

Biastoch, A., C. W. Boening, J. Getzlaff, J.-M. Molines, and G. Madec (2008), Causes of interannual-decadal variability in the meridional overturning circulation of the midlatitude North Atlantic Ocean, *J. Clim.*, *21*(24), 6599–6615, doi:10.1175/2008JCLI2404.1.

Cabanes, C., T. Lee, and L.-L. Fu (2008), Mechanisms of interannual variations of the meridional overturning circulation of the North Atlantic Ocean, *J. Phys. Oceanogr.*, *38*(2), 467–480, doi:10.1175/2007JPO3726.1.

Chylek, P., C. Folland, L. Frankcombe, H. Dijkstra, G. Lesins, and M. Dubey (2012), Greenland ice core evidence for spatial and temporal variability of the Atlantic Multidecadal Oscillation, *Geophys. Res. Lett.*, *39*, L09705, doi:10.1029/2012GL051241.

Collins, M., et al. (2013), Chapter 12: Long-term climate change—Projections, commitments and irreversibility, in *Climate Change 2013: The Physical Science Basis. Contribution of Working Group I to the Fifth Assessment Report of the Intergovernmental Panel on Climate Change*, edited by T. F. Stocker et al., pp. 1029–1136, Cambridge Univ. Press, Cambridge, U. K., and New York.

Dai, A., A. Hu, G. Meehl, W. Washington, and W. Strand (2005), Atlantic thermohaline circulation in a coupled general circulation model: Unforced variations versus forced changes, *J. Clim.*, *18*(16), 3270–3293, doi:10.1175/JCLI3481.1.

Danabasoglu, G. (2008), On multidecadal variability of the Atlantic meridional overturning circulation in the community climate system model version 3, *J. Clim.*, *21*(21), 5524–5544, doi:10.1175/2008JCLI2019.1.

Delworth, T., S. Manabe, and R. Stouffer (1993), Interdecadal variations of the thermohaline circulation in a coupled ocean-atmosphere model, *J. Clim.*, *6*(11), 1993–2011, doi:10.1175/1520-0442(1993)006<1993:IVOTTC>2.0.CO;2.

Dickson, R. R., J. Meincke, S.-A. Malmberg, and A. J. Lee (1988), The "great salinity anomaly" in the northern North Atlantic 1968–1982, *Prog. Oceanogr.*, *20*(2), 103–151.

Dong, B., and R. Sutton (2005), Mechanism of interdecadal thermohaline circulation variability in a coupled ocean-atmosphere GCM, *J. Clim.*, *18*(8), 1117–1135.

Duchez, A., et al. (2014), A new index for the Atlantic Meridional Overturning Circulation at 26°N, *J. Clim.*, *27*(17), 6439–6455.

Dufresne, J.-L., et al. (2013), Climate change projections using the IPSL-CM5 Earth System Model: From CMIP3 to CMIP5, *Clim. Dyn.*, *40*(9–10), 2123–2165, doi:10.1007/s00382-012-1636-1.

Dunstone, N., D. Smith, and R. Eade (2011), Multi-year predictability of the tropical Atlantic atmosphere driven by the high latitude North Atlantic Ocean, *Geophys. Res. Lett.*, *38*, L14701, doi:10.1029/2011GL047949.

Eden, C., and J. Willebrand (2001), Mechanism of interannual to decadal variability of the North Atlantic circulation, *J. Clim.*, *14*(10), 2266–2280, doi:10.1175/1520-0442(2001)014<2266:MOITDV>2.0.CO;2.

Escudier, R., J. Mignot, and D. Swingedouw (2013), A 20-year coupled ocean-sea ice-atmosphere variability mode in the North Atlantic in an AOGCM, *Clim. Dyn.*, *40*(3–4), 619–636.

Frankcombe, L. M., A. von der Heydt, and H. A. Dijkstra (2010), North Atlantic multidecadal climate variability: An investigation of dominant time scales and processes, *J. Clim.*, *23*(13), 3626–3638, doi:10.1175/2010JCLI3471.1.

Gelderloos, R., C. A. Katsman, and S. S. Drijfhout (2011), Assessing the roles of three eddy types in restratifying the Labrador Sea after deep convection, *J. Phys. Oceanogr.*, *41*(11), 2102–2119.

Good, S. A., M. J. Martin, and N. A. Rayner (2013), EN4: Quality controlled ocean temperature and salinity profiles and monthly objective analyses with uncertainty estimates, *J. Geophys. Res. Oceans*, *118*, 6704–6716, doi:10.1002/2013JC009067.

Grotzner, A., M. Latif, and T. Barnett (1998), A decadal climate cycle in the North Atlantic Ocean as simulated by the ECHO coupled GCM, *J. Clim.*, *11*(5), 831–847, doi:10.1175/1520-0442(1998)011<0831:ADCCIT>2.0.CO;2.

Huang, W., et al. (2014), Variability of Atlantic meridional overturning circulation in FGOALS-g2, *Adv. Atmos. Sci.*, *31*(1), 95–109.

Jungclaus, J., H. Haak, M. Latif, and U. Mikolajewicz (2005), Arctic-North Atlantic interactions and multidecadal variability of the meridional overturning circulation, *J. Clim.*, *18*(19), 4013–4031.

Kelly, B. C. (2007), Some aspects of measurement error in linear regression of astronomical data, *Astrophys. J.*, *665*(2), 1489–1506.

Knutti, R., D. Masson, and A. Gettelman (2013), Climate model genealogy: Generation CMIP5 and how we got there, *Geophys. Res. Lett.*, *40*, 1194–1199, doi:10.1002/grl.50256.

Liu, Z. (2012), Dynamics of interdecadal climate variability: A historical perspective, *J. Clim.*, *25*(6), 1963–1995.

Madec, G. (2008), Nemo ocean engine: Note du pole de modélisation, Institut Pierre-Simon Laplace (IPSL), France, No 27 ISSN No 1288–1619, *Tech. Rep.*, IPSL LSCE, UVSQ, CEA CNRS, Unite Mixte, Bat 712, F–91191 Gif Sur Yvette, France. [Available at http://www.nemo-ocean.eu.]

Marzocchi, A., J. J.-M. Hirschi, N. P. Holliday, S. A. Cunningham, A. T. Blaker, and A. C. Coward (2015), The North Atlantic subpolar circulation in an eddy-resolving global ocean model, *J. Mar. Syst.*, *142*, 126–143, doi:10.1016/j.jmarsys.2014.10.007.

McCarthy, G. D., D. A. Smeed, W. E. Johns, E. Frajka-Williams, B. I. Moat, D. Rayner, M. O. Baringer, C. S. Meinen, J. Collins, and H. L. Bryden (2015), Measuring the Atlantic meridional overturning circulation at 26°N, *Prog. Oceanogr.*, *130*, 91–111.

Medhaug, I., H. Langehaug, T. Eldevik, T. Furevik, and M. Bentsen (2012), Mechanisms for decadal scale variability in a simulated Atlantic meridional overturning circulation, *Clim. Dyn.*, *39*(1–2), 77–93, doi:10.1007/s00382-011-1124-z.

Menary, M. B., W. Park, K. Lohmann, M. Vellinga, M. D. Palmer, M. Latif, and J. H. Jungclaus (2012), A multimodel comparison of centennial Atlantic meridional overturning circulation variability, *Clim. Dyn.*, *38*(11–12), 2377–2388, doi:10.1007/s00382-011-1172-4.

Pohlmann, H., D. M. Smith, M. A. Balmaseda, N. S. Keenlyside, S. Masina, D. Matei, W. A. Muller, and P. Rogel (2013), Predictability of the mid-latitude Atlantic meridional overturning circulation in a multi-model system, *Clim. Dyn.*, *41*(3–4), 775–785, doi:10.1007/s00382-013-1663-6.

Robson, J., R. Sutton, K. Lohmann, D. Smith, and M. D. Palmer (2012), Causes of the rapid warming of the North Atlantic Ocean in the mid-1990s, *J. Clim.*, *25*(12), 4116–4134.

Robson, J. I. (2010), Understanding the performance of a decadal prediction system, PhD thesis, Univ. of Reading, Reading, U. K.

Scaife, A. A., D. Copsey, C. Gordon, C. Harris, T. Hinton, S. Keeley, A. O'Neill, M. Roberts, and K. Williams (2011), Improved Atlantic winter blocking in a climate model, *Geophys. Res. Lett.*, *38*, L23703, doi:10.1029/2011GL049573.

Sévellec, F., and A. V. Fedorov (2013), The leading, interdecadal eigenmode of the Atlantic meridional overturning circulation in a realistic ocean model, *J. Clim.*, *26*(7), 2160–2183.

Sicre, M.-A., P. Yiou, J. Eiriksson, U. Ezat, E. Guimbaut, I. Dahhaoui, K.-L. Knudsen, E. Jansen, and J.-L. Turon (2008), A 4500-year reconstruction of sea surface temperature variability at decadal time-scales off North Iceland, *Quat. Sci. Rev.*, *27*(21–22), 2041–2047, doi:10.1016/j.quascirev.2008.08.009.

Swingedouw, D., P. Ortega, J. Mignot, E. Guilyardi, V. Masson-Delmotte, P. G. Butler, M. Khodri, and R. Séférian (2015), Bidecadal North Atlantic Ocean circulation variability controlled by timing of volcanic eruptions, *Nat. Commun.*, *6*, 6545.

Taylor, K. E., R. J. Stouffer, and G. A. Meehl (2012), An overview of CMIP5 and the experiment design, *Bull. Am. Meteorol. Soc.*, *93*(4), 485–498.

Walters, D., et al. (2011), The Met Office unified model global atmosphere 3.0/3.1 and JULES global land 3.0/3.1 configurations, *Geosci. Model Dev. Discuss.*, *4*(2), 1213–1271.

Williams, K., et al. (2015), The Met Office global coupled model 2.0 (GC2) configuration, *Geosci. Model Dev. Discuss.*, *8*(1), 521–565.

Zhang, L., and C. Zhao (2015), Processes and mechanisms for the model SST biases in the North Atlantic and North Pacific: A link with the Atlantic meridional overturning circulation, *J. Adv. Model. Earth Syst.*, *7*, doi:10.1002/2014MS000415, in press.